Discrete Element Method for Simulation and Calibration of Cotton Stalk Contact Parameters

Jiali Li,[a] Yongtao Lu,[c] Xiangbin Peng,[a] Peng Jiang,[a] Bingcheng Zhang,[a] Lanyu Zhang,[a] Hewei Meng,[a,*] Za Kan,[a,*] and Xinzhong Wang [b]

To improve the accuracy of the discrete element research, physical and simulation experiments were used to calibrate the cotton stalk contact parameters. Based on the stalk-stalk and stalk-steel contact mechanics, the parameters were measured in physical experiments, and the discrete element simulation software was used to build the stalk model. In the simulation process, the Plackett-Burman experiment was used to screen three significant factors from six initial factors. The steepest Plackett-Burman experiment was used to determine the optimal interval of the significant factors. A second-order regression model of the significant factors and the angle of repose was established according to the Central Composite design experiment. The best parameter combination of the significant factors was then obtained: the coefficient of static friction on stalk-steel contact was 0.31, the coefficient of static friction on stalk-stalk contact was 0.62, and the coefficient of rolling friction on stalk-stalk contact was 0.02. The relative error between the physical angle of repose and the simulated angle was 3.27%, indicating that it is feasible to apply the simulation experiment instead of the physical one. It offers insights into cotton stalk contact parameter settings and film-stalk separation in the simulation.

DOI: 10.15376/biores.18.1.400-416

Keywords: Cotton stalk; Discrete element simulation; Parameter calibration; Angle of repose

*Contact information: a: College of Mechanical and Electrical Engineering, Shihezi University, Shihezi, 832000, P.R. China; b: School of Agricultural Equipment Engineering, Jiangsu University, Zhenjiang, 212013, P.R. China; c: Institute of Machinery and Equipment, Xinjiang Academy of Agricultural Reclamation, Shihezi, 832000, P.R. China; *Corresponding author: kz-shz@163.com; mhw_mac@shzu.edu.cn*

INTRODUCTION

Polyethylene mulching is an important measure of cotton yield enhancement. The mulch film is laid before cotton sowing and recovered after harvest every year. Agricultural mulch film has poor mechanical properties and breaks severely after the tillage period, forming a residual film. Residual film is a plastic waste, which is not easy to decompose. The accumulation of residual film in soil will change the physical and chemical properties of the soil, which is a threat to the surrounding ecology (Hu *et al.* 2019). If the recovered film is not promptly dealt with, it will also pollute the air and soil environment (Hu *et al.* 2019). Currently, the main problem that restricts the resource utilization of residual film is the high content of impurities. Cotton stalk is the main component in the mixture of residual film and impurities. Thus, it is particularly important to explore the movement law of cotton stalk in the separation process for the design of separation device.

In recent years, discrete element simulation software has become more and more widely used in the field of agricultural materials (Boac *et al.* 2010; Petingco *et al.* 2020). Numerically simulating the film stalk separation process by using this method is helpful to reveal the film stalk screening mechanism (Gao *et al.* 2017; Chen *et al.* 2019). To improve the accuracy of the discrete element model of cotton stalk, it is necessary to define the intrinsic parameters and contact parameters precisely (Zhang *et al.* 2019; Nguyen *et al.* 2021). The contact parameters mainly include the coefficient of static friction, the coefficient of rolling friction, and the coefficient of restitution (Coetzee 2020; Ma *et al.* 2020).

Many researchers have used the discrete element method to calibrate the material contact parameters, mainly in the research of crop stalks and seeds. In terms of crop stalks, Zhang *et al.* (2018) used the bucket-discharged method to measure the angle of repose of the corn stalks and used the orthogonal experiment to calibrate the contact parameters. Liao *et al.* (2020) used the cylinder lifting method to measure the angle of repose of the forage rape stalks. The contact parameters were calibrated by combining the two-level factor experiment and the response surface experiment. Wang *et al.* (2022) used the Plackett-Burman and the Box-Behnken Design experiments to calibrate the parameters of alfalfa based on the angle of repose. Zhang *et al.* (2020) calibrated the key parameters of the corn stalks crushing process based on the Hertz-Mindlin with bonding contact model. In terms of seeds, the contact parameters of castor bean capsules were calibrated by establishing a three-dimensional model and using the discrete element method to design a Central Composite Design experiment (Hou *et al.* 2019). Virtual design of experiment (DOE) was used to change corn contact parameters for simulation calibration (Mohammad *et al.* 2017).

The above-mentioned studies showed that the application of the discrete element methods to agricultural materials has been explored extensively. However, few studies have been done on cotton stalk. The cotton stalk is severely lignified and shows significant differences in material properties from the stalk of crops such as corn, forage rape, and sugarcane. Therefore, the calibration of contact parameters is important when using the discrete element method for the cotton stalk motion process study.

In this study, the cotton stalk of Xinluzao No.83 variety was selected as the research object. The relevant contact parameters of the stalk were measured through physical experiments. The angle of repose of the stalk was obtained by the bucket-discharged experiment, and the relative error of the angle was used as the response index. The discrete element method was used to study the mechanical contact characteristics of stalk-stalk and stalk-steel. The contact parameters in the Experts in Discrete Element Modeling (EDEM) software were calibrated through the Plackett-Burman, the steepest Plackett-Burman, and the Central Composite Design experiments. The calibrated cotton stalk contact parameters can be used for the discrete element method to simulate the movement law of cotton stalks on the separation device.

MATERIALS AND METHODS

Physical Experiments

Xinluzao No. 83, one of the cotton varieties grown in Xinjiang, was used as the research material. The experimental cotton stalks were sampled from a cotton field at Shihezi University, Xinjiang and stored in the natural state after manual harvesting in autumn. The sampling site was near the middle and lower parts of the cotton plant, about

10 cm above the stubble. About 500 stalks were cut with pruning shears (Xiong Yue San Huan Horticulture tools Co., Ltd, Liaoning, China). They were characterized by a uniform length of 80 mm for straight and disease-free branches. The digital Sartorius MA100d electronic moisture analyzer (Sartorius, Göttingen, Germany) was used to measure the moisture content. The moisture content accuracy of the analyzer was 0.01%, and the quality accuracy was 0.001 g. The average moisture content of the stalks was 17.74%. The digital vernier caliper with an accuracy of 0.02 mm was used to measure the stalk diameters. The average diameters of the upper, middle, and lower ends of the stalks were 9.05 mm, 9.33 mm, and 9.38 mm, respectively.

Cotton stalk physical properties

The coefficient of static friction μ_s of the cotton stalk was determined by the inclined method (Gu *et al.* 2017), and the instrument was a friction angle tester (Shihezi Univesity, China), as shown in Fig. 1. Two stalks were fixed as a group as the experimental object (Zhang *et al.* 2017). To avoid gaps between the experimental stalks and the contact surface, the difference in the average diameter of the same group was required to be less than 5%. The coefficient of static friction on stalk-steel contact $\mu_s(k\text{-}l)$ was measured when the contact surface was steel. The coefficient of static friction on stalk-stalk contact $\mu_s(k\text{-}k)$ was measured when the contact surface was stalk bark. The bark was peeled off from the cotton stalk and pasted on the surface of the inclined plane of the friction angle tester. During the experiment, a set of samples were placed on the upper part of the inclined plane. The inclination angle of the plate was gradually increased by turning the handwheel. When the stalk sample was slightly moved, the angle of the plane at this moment was recorded as the sliding friction angle. According to Eq. 1, $\mu_s(k\text{-}l)$ and $\mu_s(k\text{-}k)$ were calculated (Wen *et al.* 2017). The experiment was repeated 50 times, and the average of the calculation results was taken. Here is the expression of Eq. 1,

$$\tan(\alpha) = f \quad (1)$$

where α is the sliding friction angle (°), and f is the coefficient of static friction.

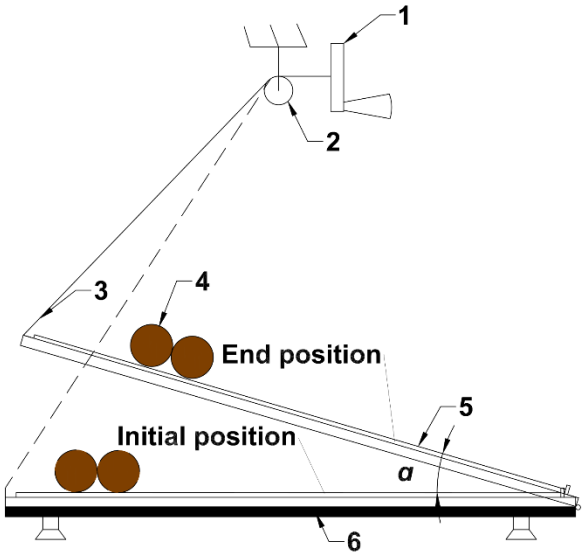

Fig. 1. The tester of angle of friction: 1: Handwheel; 2: Lifting device; 3: Tow rope; 4: Cotton stalk samples; 5: Replaceable board; 6: Base

The device for measuring the coefficient of rolling friction μ_k of cotton stalk was the same as the coefficient of static friction μ_s. The difference between the measurement methods was that the former was measured with a single cotton stalk (Wen *et al.* 2020a). To reduce the influence of the burrs at both ends of the cut stalk on the rolling, the burrs were lightly polished off with sandpaper. The friction angle tester was adjusted to the horizontal state, the stalk sample was placed on the tester, and the inclination angle of the tester was changed. The angle was recorded as the rolling friction angle when the stalk sample started to roll. The experiment was repeated 50 times, and the average value was taken.

The coefficient of restitution on stalk-steel contact $\mu_r(k\text{-}l)$ and that on stalk-stalk contact $\mu_r(k\text{-}k)$ were measured, as shown in Fig. 2. The $\mu_r(k\text{-}l)$ and $\mu_r(k\text{-}k)$ were calculated by simplified Eq. 2 (Liu *et al.* 2020; Wang *et al.* 2020). Here is the expression of Eq. 2,

$$e = \sqrt{\frac{S_2}{S_1}} \tag{2}$$

where e is the coefficient of restitution, S_1 is the initial drop height of sample (mm), and S_2 is the rebound height of sample (mm).

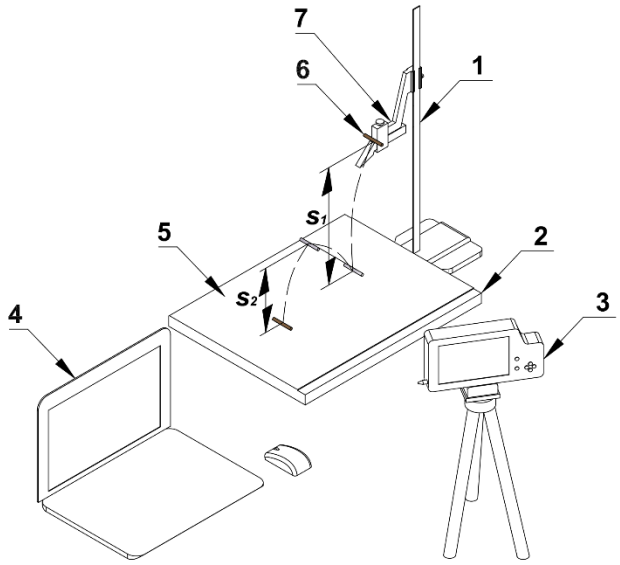

Fig. 2. The measurement device of the coefficient of restitution: 1: Movable height gauge; 2: Collision base; 3: High-speed camera; 4: PC-Computer; 5: Replaceable collision contact surface; 6: Cotton stalk sample; 7: Loading platform. Note: S_1 is the initial drop height of sample (mm), and S_2 is the rebound height of sample (mm).

When the stalks fall, the windward area is small and the speed is fast, and the air resistance can be ignored. Five release heights of 300, 350, 400, 450, and 500 mm were selected. Each stalk sample was placed on the measuring device and parallel to the outer edge of the release table. According to the requirements of measuring $\mu_r(k\text{-}l)$ and $\mu_r(k\text{-}k)$, the falling plane was evenly laid with corresponding materials to ensure that the cotton stalk contact surface was flat. When the sample was in free fall, the high-speed camera (Fastec Imaging, FASTEC TS4, USA) was used to shoot its trajectory. The initial drop height and rebound height of the sample were recorded, named, and stored. High-speed camera analysis software ProAnalys (Fastec Imaging, FASTEC TS4, USA) was used to process the experiment data. The height ruler was taken as the reference system. When the

cotton stalk was at the initial height, its projection center on the contact surface was taken as the origin. The X-Y coordinate system was established to obtain the movement trajectory of the sample's falling rebound over time. The coordinate values in the high-speed camera analysis software were imported into the Origin 2019b software (OriginLab, Northampton, MA, USA). The time-displacement image of the cotton stalk falling process was obtained. The experiment was repeated 5 times at each height to find the average value.

Angle of repose experiment

The angle of repose was measured by the bucket-discharged method, which was similar to the method used in the study by Mohammad *et al.* (2017). The length of the stalks was 80 mm. Based on this, a device with a steel extractable gate was designed, as shown in Fig. 3. The device was made of plexiglass, with a steel plane 400 mm long and 100 mm wide at the bottom, surrounded by plexiglass panels with a height of 200 mm, and equipped with gate slots. The gate was inserted, and the device was filled with the stalks. When the gate was removed, the stalks moved. After the stalks stopped moving, the angle between the inclined surface of the stalk material flow and the bottom surface was seen as the angle of repose. The experimental results were photographed by the camera and processed by Matlab R2015b software (Mathworks, Massachusetts, USA). The digital image tool of Origin 2019b was used to delimit the pixel value range of the image, extract the boundary curve, perform linear fitting, calculate the slope of the fitted curve, and obtain the angle values (Wen *et al.* 2020b; Yu *et al.* 2020). The experiment was carried out 20 times, and the average value was taken.

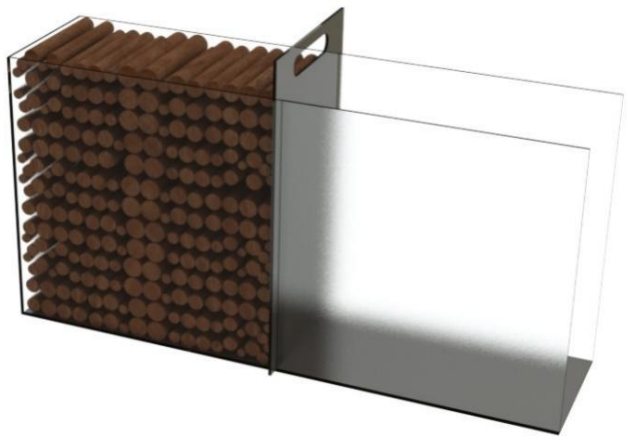

Fig. 3. The measuring instrument of angle of repose

Simulation Experiments

A method that combined the physical and simulation experiments was used to calibrate the cotton stalk contact parameters. The angle of repose θ of the cotton stalks was measured by the bucket-discharged method (Tekeste *et al.* 2018). The EDEM 2021 software (Altair, Troy, Mich., USA) was used to simulate the angle. The Design-Expert 8.0.6 software (Stat Ease Inc., Minneapolis, USA) was used to design the Plackett-Burman experiment, the steepest Plackett-Burman experiment, and the Central Composite Design experiment. Through the Plackett-Burman experiment, the significant factors were determined. Through the steepest Plackett-Burman experiment, the level range of the significant factors was narrowed. The optimal parameter combination of the significant factor was obtained through the Central Composite Design experiment. The angle under

the optimal combination was compared with the physical. Then, the simulation experiment was optimized.

Modeling and parameter setting

Firstly, the standard single sphere particles were selected as the basic unit of the discrete element model of the cotton stalk. The particle radius was 1.0 mm. The stalk model was formed by stacking 40 particle layers, with an angle difference of 30° between the particle positions of two adjacent layers. Each particle layer contained 18 single-sphere particles (Fig. 4). The x-axis, y-axis, and z-axis coordinate positions of these 720 particles were calculated and input into EDEM 2021 software to generate a cylindrical model with a diameter of 10 mm and a length of 80 mm. The basic parameters of the model were set according to the intrinsic parameters of the cotton stalk, as shown in Table 1 (Jiang *et al.* 2019). Secondly, the angle of repose measurement device model was imported into EDEM 2021 software, and its material property was steel. The basic parameters of the device model were set according to the steel. The particle factory was established in the device model, and the number of stalk model was set to 454.

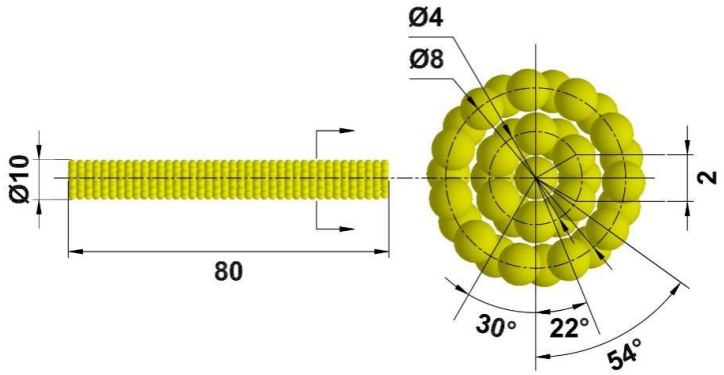

Fig. 4. Discrete element model of cotton stalk. Note: The unit for all numbers was mm.

Table 1. Material Parameter Settings of Discrete Element Method Simulation

Material	Parameter	Value
Cotton stalks	Poisson's Ratio	0.35
	Shear Modulus (Pa)	1.0×10^{6}
	Density ($kg.m^{-3}$)	120
Steel	Poisson's Ratio	0.30
	Shear Modulus (Pa)	1.0×10^{10}
	Density ($kg.m^{-3}$)	7850

Then, the contact parameters were set according to the experiment scheme. The Hertz-Mindlin contact model is one of the most commonly used models to simulate the behavior of non-viscous particles. The Hertz-Mindlin (no-slip) contact model is a nonlinear spring elastic model without cohesion. Therefore, it was selected for the stalk-stalk and stalk-steel contact model. The body-centered cubic form (bcc) was selected for the accumulation of stalks. The Rayleigh time step was set to 35 %, the simulation time was 50 s, the extraction speed was 50 mm/s (Hou *et al.* 2019), and the extraction start time was 15 s. Finally, the simulation started. After the extraction of the gate, the stalks changed from a static stable state to a natural accumulation state and formed an angle.

In EDEM 2021 software, the color was used to represent the movement change of the stalk models, and the blue indicated that the models were in a static state, as shown in Fig. 5. The figure was saved, and the accumulation angle was extracted through the Matlab R2015b software to obtain the angle of repose.

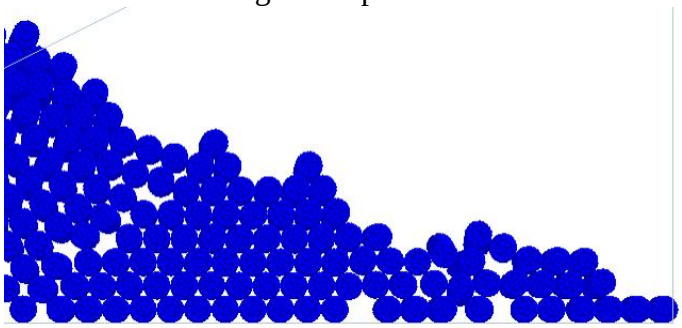

Fig. 5. The natural accumulation state of the cotton stalk model

Plackett-Burman experiment

The Plackett-Burman experiment is a screening design experiment. It is suitable for experimental design under the condition of many experimental factors, aiming to screen out the factors that have significant influence. The six contact parameters to be screened were: the coefficient of static friction on stalk-steel contact μ_s*(k-l)*, the coefficient of static friction on stalk-stalk contact μ_s*(k-k)*, the coefficient of rolling friction on stalk-steel contact μ_k*(k-l)*, the coefficient of rolling friction on stalk-stalk contact μ_k*(k-k)*, the coefficient of restitution on stalk-steel contact μ_r*(k-l)*, and the coefficient of restitution on stalk-stalk contact μ_r*(k-k)*. Three parameters, which had significant effects on the response value, were selected.

The experimental factors and levels were set as shown in Table 2. In the Plackett-Burman experiment, the selection of the levels of the factors is not clearly defined, and the appropriate level can be set according to the actual situation. The length of the cotton stalk model was 80 mm, and the contact area with the device material was large. The model was composed of multiple spherical particles, which had increased surface roughness compared to the actual one. Therefore, the range of parameter levels was set based on 0.5 to 1.1 times the measured average value. In total, two levels and three center points were set, and 15 experiments were performed.

Table 2. Plackett-Burman Experimental Factors and Levels

Symbol	Parameter	Low level (-1)	High level (-1)
A	Coefficient of restitution on stalk-stalk contact μ_r*(k-k)*	0.14	0.32
B	Coefficient of static friction on stalk-stalk contact μ_s*(k-k)*	0.33	0.72
C	Coefficient of rolling friction on stalk-stalk contact μ_k*(k-k)*	0.06	0.12
D	Coefficient of restitution on stalk-steel contact μ_r*(k-l)*	0.22	0.49
E	Coefficient of static friction on stalk-steel contact μ_s*(k-l)*	0.24	0.52
F	Coefficient of rolling friction on stalk-steel contact μ_k*(k-l)*	0.05	0.1
G、*H*、*I*、*J*、*K*	Virtual parameters		

Steepest Plackett-Burman experiment

To make the level of each factor approach the area near the optimal value as soon as possible, the steepest Plackett-Burman experiment was carried out based on the Plackett-Burman experiment. In this design, three factors were set. The level of significant factors was centered on the measured average value, and five levels were set in equal steps. The coefficient of rolling friction on stalk-stalk contact μ_k*(k-k)* was larger than the reference value (Jiang *et al.* 2019), so the lowest level of the Plackett-Burman simulation experiment was set as the center, and five levels were set with equal steps. The non-significant factor level was set according to the average value of the physical measured contact parameters, and the simulation experiment was performed with the angle of repose of physical experiment θ_s as the experimental index. A total of five experiments were performed.

Central Composite Design experiment

The Central Composite Design experiment was used to obtain the optimal parameter combination. The optimal area of each significant factor was determined through the steepest Plackett-Burman experiment, and five levels of significant experimental factors with this area were set as the center. The average value of the physical experiment was taken as the non-significant factors, and six center points were used to carry out the Central Composite Design experiment. A total of 20 experiments were performed. The response surface analysis was carried out, the regression equations of factors and response values were obtained, and optimal combination prediction of significant factors was made.

RESULTS AND DISCUSSION

Cotton Stalk Physical Properties

The sliding friction angles of stalk-steel and stalk-stalk were 25.32° and 32.89°, respectively. Correspondingly, the coefficient of static friction on stalk-steel contact μ_s*(k-l)* and that on stalk-stalk contact μ_s*(k-k)* were 0.47 and 0.65.

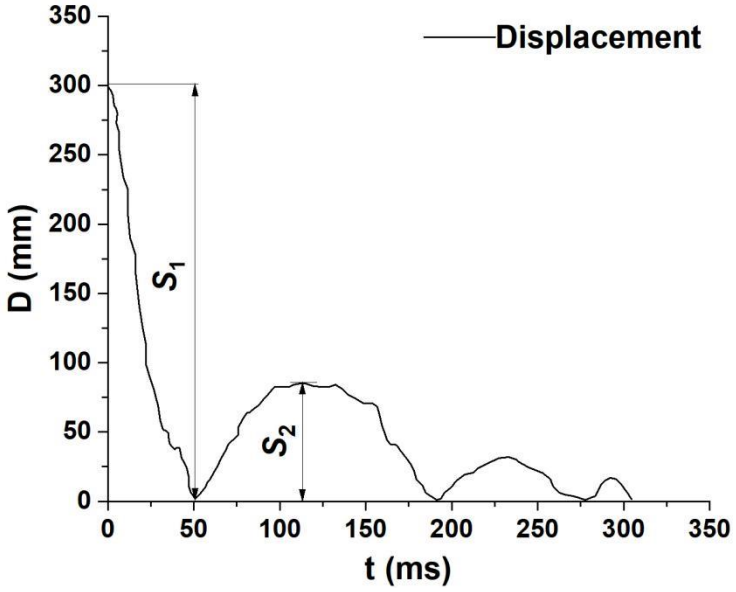

Fig. 6. Time-displacement curve of cotton stalks movement

Angle of Repose Experiment

The image of the angle of repose was obtained. The Matlab R2015b software was used to process the original image with gray scale and binarization. The holes were filled, and the stalk boundary curve was extracted, as shown in Fig. 7.

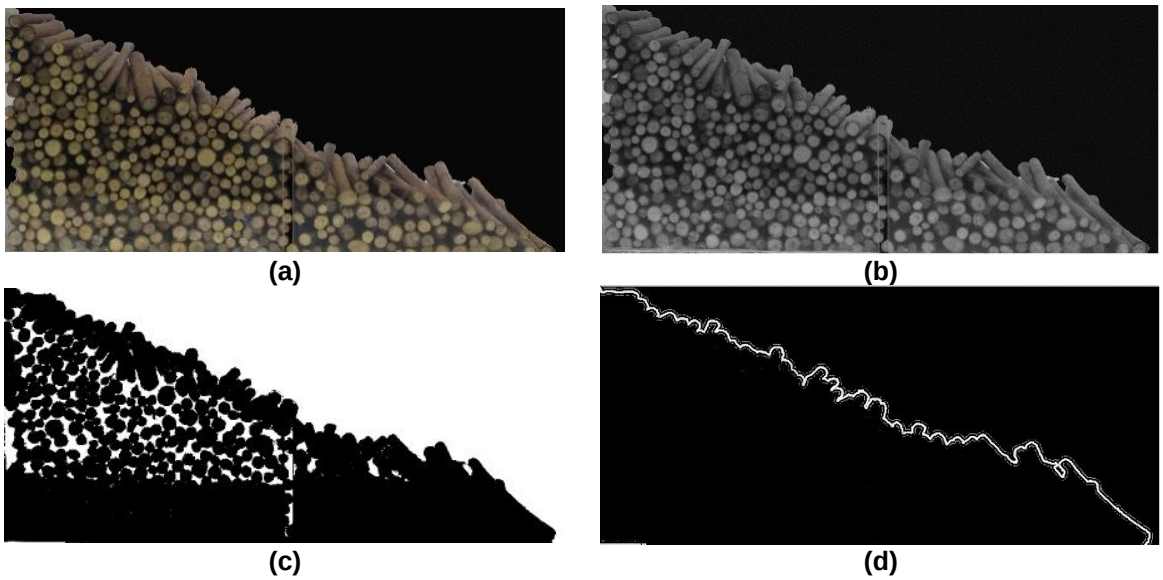

Fig. 7. The angle of repose of the cotton stalk image processing steps: (a): original image; (b): gray processing; (c) binarization processing; and (d): hole filling

Figure 8 is an example of fitting curve, and the angle between the fitting curve and the horizontal axis is the angle of repose. The average value of θ_p obtained was 24.79°.

The governing factors for the angle of repose were analyzed. In the initial state, the cotton stalks were in a stable and static state under the action of the side wall and the gate. The stalks in contact with the gate were directly subjected to the side pressure of the gate. The stalks without contact with the gate were indirectly subjected to the lateral pressure. The effect of the pressure existed in the form of lateral extrusion of the stalks to stalks, and gradually weakened in the direction far from the gate (L was close to zero). When the gate was evacuated, the side pressure disappeared, and the stalks moved under the action of downward gravity, lateral inertia, and friction between materials until the force was balanced. At this time, the stalks stopped moving and formed the angle.

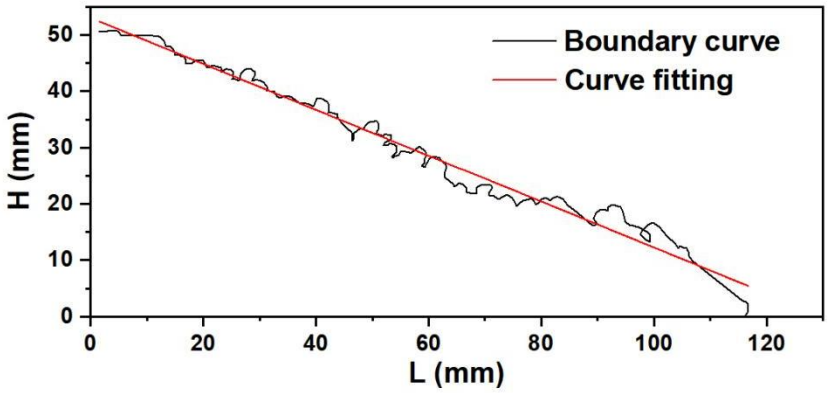

Fig. 8. Linear fitting by using Origin 2019b software

Plackett-Burman Experiment

The codes and results of the Plackett-Burman experiment factors are shown in Table 3, and the analysis of variance (ANOVA) of the experimental factors are shown in Table 4. From the ANOVA results in Table 4, the P-values for the coefficient of rolling friction on stalk-stalk contact μ_k*(k-k)* (*C*), the coefficient of static friction on stalk-steel contact μ_s*(k-l)* (*E*), and the coefficient of static friction on stalk-stalk contact μ_s*(k-k)* (*B*) were less than 0.05, which were all significant factors.

Table 3. Design and Results of Plackett-Burman Experiment

Experiment No.	Factors						Angle of Repose θ_s (°)
	A	*B*	*C*	*D*	*E*	*F*	
1	1	-1	1	1	1	-1	35.75
2	-1	1	1	1	-1	-1	38
3	-1	-1	-1	-1	-1	-1	23
4	-1	1	-1	1	1	-1	35
5	0	0	0	0	0	0	30.96
6	1	1	-1	1	1	1	30
7	-1	-1	-1	1	-1	1	29
8	1	1	1	-1	-1	-1	29.26
9	1	-1	-1	-1	1	-1	29.62
10	-1	1	1	-1	1	1	42.62
11	1	-1	1	1	-1	1	29.26
12	0	0	0	0	0	0	30.96
13	-1	-1	1	-1	1	1	30.6
14	1	1	-1	-1	-1	1	27.92
15	0	0	0	0	0	0	29.25

Table 4. ANOVA of Plackett-Burman Experiment

Error Source	Square	F	P
A	22.44	2.39	0.1606NS
B	54.49	5.81	0.0425*
C	79.83	8.51	0.0194*
D	16.31	1.74	0.2239NS
E	61.43	6.55	0.0337*
F	0.13	0.013	0.9106NS
Note: *Denotes the significant influence of factors (P ≤ 0.05); NS denotes the non-significant influence of factors (*P* > 0.05).			

Steepest Plackett-Burman Experiment

As shown in Table 5, the coefficient of rolling friction on stalk-stalk contact μ_k*(k-k)*, the coefficient of static friction on stalk-steel contact μ_s*(k-l)*, and the coefficient of static friction on stalk-stalk contact μ_s*(k-k)* decreased with their respective levels. The relative error between the simulated value and the physical value of the angle of repose θ was also reduced. The error was reduced to the lowest in the No. 4 experiment, and the result was 12.5%. Therefore, the center points of μ_k*(k-k)*, μ_s*(k-l)*, and μ_s*(k-k)* were set to 0.04, 0.37, and 0.55, respectively, and the Central Composite Design experiment was performed.

Table 5. Design and Results of Steepest Plackett-Burman Experiment

Experiment No.	Coefficient of Rolling Friction on Stalk-Stalk Contact $\mu_k(k\text{-}k)$	Coefficient of Static Friction on Stalk-Steel Contact $\mu_s(k\text{-}l)$	Coefficient of Static Friction on Stalk-Stalk Contact $\mu_s(k\text{-}k)$	Angle of Repose θ_s (°)	Relative Error (%)
1	0.1	0.67	0.85	36.5	46.6
2	0.08	0.57	0.75	32.54	31.32
3	0.06	0.47	0.65	30.5	23
4	0.04	0.37	0.55	27.9	12.5
5	0.02	0.27	0.45	22.78	16.1

Central Composite Design Experiment

Experiment results

The level of each experimental factor is shown in Table 6, and other levels were set according to the default values of Design-expert 8.0.6 software. A three-factor five-level Central Composite Design experiment was carried out, and six central points were selected for a total of 20 groups of experiments. Table 6 is the Central Composite Design experimental factor level setting, and Table 7 is the Central Composite Design experiment design and results.

Table 6. Central Composite Design Experiment Factors and Levels

Symbol	Parameter	Low Level (-1)	High Level (-1)
a	Coefficient of static friction on stalk-steel contact $\mu_s(k\text{-}l)$	0.27	0.47
b	Coefficient of static friction on stalk-stalk contact $\mu_s(k\text{-}k)$	0.45	0.65
c	Coefficient of rolling friction on stalk-stalk contact $\mu_k(k\text{-}k)$	0.02	0.06
Y	Angle of repose θ_s		

Table 7. Design and Results of Central Composite Design Experiment

Experiment No.	Code			Response Value
	a	*b*	*c*	*Y*
1	1	1	-1	27.47
2	-1	-1	-1	29.25
3	0	0	0	26.57
4	0	0	0	23.64
5	0	0	0	25.27
6	0	0	0	25.81
7	1.682	0	0	31.8
8	0	-1.682	0	27.92
9	1	1	1	40.36
10	0	1.682	0	32.8
11	-1.682	0	0	25.64
12	-1	1	-1	27.92
13	-1	1	1	35
14	1	-1	-1	30.23
15	0	0	1.682	31.38
16	0	0	-1.682	21.8
17	0	0	0	25.68
18	-1	-1	1	27.92
19	1	-1	1	34.42
20	0	0	0	24.11

Regression model establishment and significance analysis

Table 8 shows that the *F*-value of the model was 12.28. The larger the *F*-value, the more obvious is the effect between treatments. The coefficient of variation (*CV*) was 6.22%, which indicated that the experiment had higher reliability. The *AdepPrecisior*-value was 12.715, which proved that the model had higher accuracy. The coefficient of determination R^2 of the equation was 0.9170, which was close to the upper limit of the value range of 0 to 1. The second-order regression model fitted well. The adjusted R_1^2-value was 0.8424, which was close to the value of R^2, indicating that the model was highly significant. It is considered that the model curve simulation experiment value was more authentic, and the quadratic polynomial equation of the significant factor on the angle of repose θ_s was obtained as Eq. 3,

$$Y = 25.09+1.67a+1.25b+2.85c-0.32ab+1.42ac+2.14bc+1.84a^2+2.41b^2+1.09c^2 \quad (3)$$

Table 8. ANOVA of Central Composite Design Experiment

Error source	Square Sum	Freedom	Mean Square	*F*	*P*
Model	353.36	9	39.26	12.28	0.0003**
a	37.90	1	37.90	11.86	0.0063**
b	21.50	1	21.50	6.73	0.0268*
c	111.04	1	111.04	34.74	0.0002**
ab	0.83	1	0.83	0.26	0.6223NS
ac	16.05	1	16.05	5.02	0.0490*
bc	36.59	1	36.59	11.45	0.0070**
a^2	49.03	1	49.03	15.34	0.0029**
b^2	84.70	1	84.70	26.50	0.0004**
c^2	17.17	1	17.17	5.37	0.0430*
Residual	31.96	10	3.20		
Lack of Fit	25.86	5	5.17	4.24	0.0695
Pure Error	6.10	5	1.22		
Summation	385.32	19			
R^2 = 0.9170; R_1^2 = 0.8424; *CV* = 6.22%; *AdepPrecisior* = 12.715					
Note: **Denotes the extremely significant influence factors ($P \le 0.01$); *Denotes the significant influence factors ($0.01 < P \le 0.05$); NS denotes the non-significant influence factors ($P > 0.05$).					

The P-values of the single factor items *a* and *c* and the interaction items *bc*, a^2, and b^2 were less than 0.01, which means that they had an extremely significant influence on the response value *Y*. The P-values of the single factor item *b* and the interaction items *ac* and c^2 were greater than 0.01 and less than 0.05, which had a significant influence on the response value *Y*. In the ANOVA, the smaller the P-value, the more significant the factor was. From the P-values of the above factors, the order of influence of each factor was: $c > b^2 > a^2 > a > bc > b > c^2 > ac$. The P-value of interaction item *ab* was much larger than 0.05, which was an unobvious factor to the response value *Y*. Therefore, if the non-obvious influencing factors in the second-order response model were eliminated, Eq. 3 can be changed to Eq. 4,

$$Y = 25.09+1.67a+1.25b+2.85c+1.42ac+2.14bc+1.84a^2+2.41b^2+1.09c^2 \quad (4)$$

Interaction analysis

Based on the above variance analysis, the interaction items *ac* and *bc* that had a significant influence on the response value *Y* were analyzed. When $\mu_s(k\text{-}k)$ (*b*) was set to the central level (0.55), the interaction between $\mu_s(k\text{-}l)$ (*a*) and $\mu_k(k\text{-}k)$ (*c*) was analyzed. It can be seen from Fig. 9 that as $\mu_s(k\text{-}l)$ (*a*) increased from 0.27 to 0.47, θ_s decreased first and then increased. When $\mu_s(k\text{-}l)$ (*a*) was greater than 0.32, θ_s no longer decreased. As $\mu_k(k\text{-}k)$ (*c*) increased in the range of 0.02 to 0.06, θ_s also gradually increased. The response surface curve changed faster along the $\mu_k(k\text{-}k)$ (*c*) direction. At the central level, the effect of $\mu_k(k\text{-}k)$ (*c*) on θ_s was more significant than that of $\mu_s(k\text{-}l)$ (*a*).

When $\mu_s(k\text{-}l)$ (*a*) was set to the central level (0.37), the interaction between $\mu_s(k\text{-}k)$ (*b*) and $\mu_k(k\text{-}k)$ (*c*) was analyzed. It can be seen from Fig. 10 that as $\mu_s(k\text{-}k)$ (*b*) increased in the range of 0.45 to 0.65, θ_s decreased first, and then increased. When $\mu_s(k\text{-}k)$ (*b*) was greater than 0.55, θ_s no longer decreased. As $\mu_k(k\text{-}k)$ (*c*) increased from 0.02 to 0.06, θ_s also gradually increased. The response surface curve changed faster along the $\mu_k(k\text{-}k)$ (*c*) direction. At the central level, the effect of $\mu_k(k\text{-}k)$ (*c*) on θ_s was more significant than that of $\mu_s(k\text{-}k)$ (*b*).

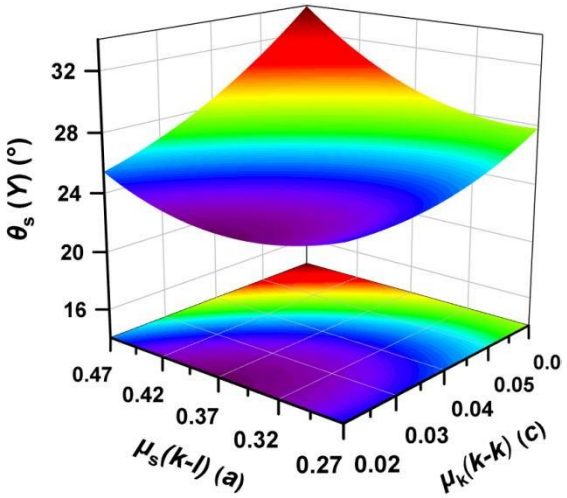

Fig. 9. Relation chart of interaction term *a* × *c* *vs*. angle of repose θ_s

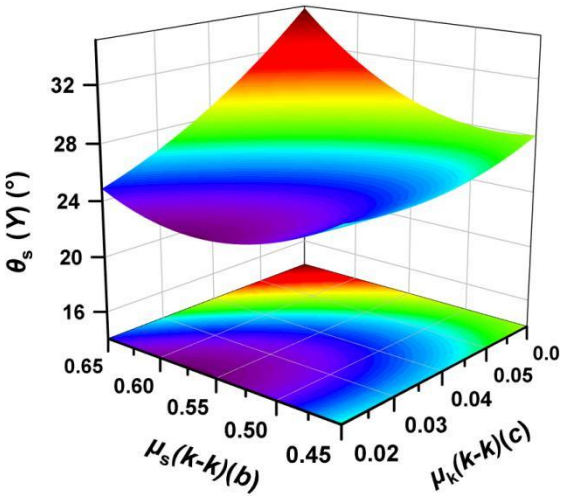

Fig. 10. Relation chart of interaction term *b* × *c* *vs*. angle of repose θ_s

Parameter Optimization and Experiment Verification

Parameter optimization

According to the experiment results, the optimization in Design-expert 8.0.6 software was used to optimize the parameter combination. The constraint conditions of each experiment factor were: the coefficient of static friction on stalk-steel contact $\mu_s(k\text{-}l)$ ranged from 0.27 to 0.47, the coefficient of static friction on stalk-stalk contact $\mu_s(k\text{-}k)$ ranged from 0.45 to 0.65, and the coefficient of rolling friction on stalk-stalk contact $\mu_k(k\text{-}k)$ ranged from 0.02 to 0.06.

The target value of response index *Y* was set to the angle of repose of physical experiment θ_p (24.79°). The optimization results of the three factors were: $\mu_s(k\text{-}l)$ was 0.31, $\mu_s(k\text{-}k)$ was 0.62, and $\mu_k(k\text{-}k)$ was 0.02. The response value of the surface of the model was better, and the predicted angle of repose was 24.41°.

Experiment verification

To verify the accuracy of the model prediction and the reliability of the parameter optimization combination, the above parameter combination was used for 3 experiments in the discrete element simulation software. The other three parameters were set according to the physical measured values. The optimal combination of experiment parameters was shown in Table 9, and the results were shown in Table 10.

Table 10 shows that the simulation results were close to the physical experiment results. The relative error between the angle of repose of simulation experiment θ_s and the angle of repose of physical experiment θ_p was less than 5%. Thus, the parameter optimization model and parameter combination were reliable, which can provide theoretical support for the discrete element simulation of cotton stalk.

Table 9. Optimal Combination of Experiment Parameters

Parameter	Value
Coefficient of static friction on stalk-steel contact μ_s*(k-l)*	0.31
Coefficient of static friction on stalk-stalk contact μ_s*(k-k)*	0.62
Coefficient of rolling friction on stalk-stalk contact μ_k*(k-k)*	0.02
Coefficient of restitution on stalk-stalk contact μ_r*(k-k)*	0.29
Coefficient of restitution on stalk-steel contact μ_r*(k-l)*	0.44
Coefficient of rolling friction on stalk-steel contact μ_k*(k-l)*	0.09

Table 10. Comparison between Model Optimization and Physical Experiment

Item	Angle of Repose θ (°)
Simulation Average	23.98
Physical Average	24.79
Relative Error	3.27%

CONCLUSIONS

1. The coefficient of restitution, the coefficient of static friction, and the coefficient of rolling friction on stalk-stalk contact were 0.29, 0.65, and 0.11, respectively. The coefficient of restitution, the coefficient of static friction, and the coefficient of rolling friction on stalk-steel contact were 0.44, 0.47, and 0.09, respectively. The angle of repose of the physical experiment was 24.79°.
2. Through the Plackett-Burman screening experiment, the coefficient of rolling friction on stalk-stalk contact, the coefficient of static friction on stalk-steel contact, and the coefficient of static friction on stalk-stalk contact had significant effects on the angle of repose of cotton stalks. The influence order of the significant factors on the angle was: coefficient of rolling friction on stalk-stalk contact > coefficient of static friction on stalk-steel contact > coefficient of static friction on stalk-stalk contact.
3. Through the Central Composite Design experiment, the coefficient of determination R^2 of the equation was 0.9170, the adjusted R_1^2-value was 0.8424, and the coefficient of variation CV was 6.22%. In addition, the P-value in the response surface experiment model of Central Composite Design was 0.0003, which was far less than 0.05, indicating that the model was feasible.

4. After optimization, the μ_s*(k-l)*, μ_s*(k-k)*, μ_k*(k-k)*, μ_r*(k-k)*, μ_r*(k-l)*, and μ_k*(k-l*) values were 0.31, 0.62, 0.02, 0.29, 0.44 and 0.09, respectively. The simulated angle of repose was 23.98°. The relative error between the physical and the simulated values was 3.27%, which was less than 5%. There was no significant difference, and the relative error was within a reasonable range, indicating that the constructed model and optimized parameter combination were reliable.

The above calibrated parameters will be applied to the simulation experiments focusing on the flow of cotton stalk, such as the separation of cotton stalk and residual film, the transportation of the cotton stalk, *etc*. Future studies about the discrete element model of residual film and the kinematic behavior analysis based on the cotton stalk model and the residual film model are in progress.

ACKNOWLEDGMENTS

The authors are grateful for the support of the Key Industry Innovation Development Support Plan of Southern Xinjiang - Grant No. 2020DB008, the Open Fund of Jiangsu Province; and the Education Ministry Co-sponsored Synergistic Innovation Center of Modern Agricultural Equipment - Grant No. XTCX2006; the Graduate Education Innovation Project of Xinjiang Uygur Autonomous Region - Grant No. Xj2021G115; and the Innovation and Entrepreneurship Training Program for College Students - Grant No. Srp20211181.

REFERENCES CITED

Boac, J. M., Casada, M. E., Maghirang, R. G., and Iii, J. (2010). "Material and interaction properties of selected grains and oilseeds for modeling discrete particles," *Trans. ASABE* 53(4), 1201-1216. DOI: 10.13031/2013.32577

Chen, M., Gong, J., and Wang, Q. (2019). "Simulation analysis and experimental verification of screw mechanism stirring barley process," *J. Yangzhou University* 22(03), 19-22. DOI: 10.19411/j.1007-824x.2019.03.005

Coetzee, C. (2020). "Calibration of the discrete element method: Strategies for spherical and non-spherical particles," *Powder Tech.* 364, 851-878. DOI: 10.1016/j.powtec.2020.01.076

Gao, G., Xie, H., and Wang, T. (2017). "EDEM simulation and experiment of pullout force of protected vegetable harvester," *Trans. Chinese Soc. Agric. Eng.* 33(23), 24-31. DOI: 10.11975/j.issn.1002-6819.2017.23.004

Gu, B., Yang, Y., Zhang, Y., and Cao, Y. (2017). "Peanut stiffness coefficient of static friction coefficient measurement," *Agric. Tech.*, 37(07), 30-32. DOI: 10.11974/nyyjs.20170431013

Hou, J., Li, J., Yao, E., Bai, J., Yang, Y., and Zhu, H. (2019). "Calibration and analysis of discrete element parameters of typical castor," *J. Shenyang Agric. University* 50(05), 565-575. DOI: 10.3969/j.issn.1000-1700.2019.05.008

Hu, C., Wang, X., Chen, X., Tang, X., Zhao, Y., and Yan, C. (2019). "Current situation and control strategies of residual film pollution in Xinjiang," *Trans. Chinese Soc. Agric. Eng.* 35(24), 223-234. DOI: 10.11975/j.issn.1002-6819.2019.24.027

Jiang, D., Chen, X., Yan, L., Mo, Y., and Yang S. (2019). "Design and experiment on spiral impurity cleaning device for profile modeling residual plastic film collector," *Trans. Chinese Soc. Agric. Machinery* 50(04), 137-145. DOI: 10.6041 /j.issn.1000-1298.2019.04.015

Liao, Y., Liao, Q., Zhou, Y., Wang, Z., Jiang, Y., and Liang, F. (2020). "Parameters calibration of discrete element model of fodder rape crop harvest in bolting stage," *Trans. Chinese Soc. Agric. Machinery* 51(06), 73-82. DOI:10.6041 /j. issn.1000-1298.2020.06.008

Liu, Y., Zong, W., Ma, L., Huang, X., Li, M., and Tang, C. (2020). "Determination of three-dimensional collision restitution coefficient of oil sunflower grain by high-speed photography," *Trans. Chinese Soc. Agric. Eng.* 36(04), 44-53. DOI: 10.11975/j.issn.1002-6819.2020.04.006

Ma, W., You, Y., Wang, D., Ying, S., and Huan, X. (2020). "Parameter calibration of alfalfa seed discrete element model based on RSM and NSGA -II," *Trans. Chinese Soc. Agric. Machinery* 51(08), 136-144. DOI: 10.6041 /j.issn.1000-1298.2020.08.015

Mohammad, M., Tekeste, M. Z., and Rosentrater, K. A. (2017). "Calibration and validation of a discrete element model of corn using grain flow simulation in a commercial screw grain auger," *Trans. ASABE* 60(4), 1403-1415. DOI: 10.13031/trans.12200

Nguyen, T. X., Le, L. M., Nguyen, T. C., Nguyen, N. T. H., Le, T. T., Pham, B. T., Le, V.M. and Ly, H. B. (2021). "Characterization of soybeans and calibration of their DEM input parameters," *Particulate Sci. Tech.* 39(5), 530-548. DOI: 10.1080/02726351.2020.1775739

Petingco, M. C., Casada, M. E., Maghirang, R. G., Fasina, O. O., and Ambrose, R. (2020). "Influence of particle shape and contact parameters on DEM-simulated bulk density of wheat," *Trans. ASABE* 63(6), 1657-1672. DOI: 10.13031/trans.13718

Tekeste, M. Z., Mousaviraad, M., and Rosentrater, K. A. (2018). "Discrete element model calibration using multi-responses and simulation of corn flow in a commercial grain auger," *Trans. ASABE* 61(5), 1743-1755. DOI: 10.13031/trans.12742

Wang, H., Wu, P., He, H., Ma, Y., Bu, K., and Xue, J. (2022). "Calibration of parameters for discrete element simulation model for Alfalfa with different moisture contents based on angle of repose test," *BioResources* 17(1), 1467-1484. DOI: 10.15376/biores.17.1.1467-1484

Wang, L., Zheng, Z., Yu, Y., Liu, T., and Zhang, Z. (2020). "Determination of the energetic coefficient of restitution of maize grain based on laboratory experiments and DEM simulations," *Powder Tech.* 362, 645-658. DOI: 10.1016/j.powtec.2019.12.024

Wen, Z., Liu, F., Zhang, S., Zhang, L., and Wang, X. (2017). "Stiffness coefficient of static friction coefficient measurement," *Agric. Tech.* 37(21), 4-6+14. DOI: 10.11974/nyyjs.20171132002

Wen, X., Yang, W., Guo, W., and Zeng, B. (2020a). "Parameter determination and validation of discrete element model of segmented sugarcane harvester for impurity removal Chinese," *J. Agric Mech.* 41(01), 12-18. DOI: 10.13733/j.jcam.issn.2095-5553.2020.01.03

Wen, X., Yuan, H., Wang, G., and Jia, H. (2020b). "Calibration method of friction coefficient of granular fertilizer by discrete element simulation," *Trans. Chinese Soc. Agric. Machinery* 51(02), 115-122+142. DOI: 10.6041 /j.issn.1000-1298.2020.02.013

Yu, Q., Liu, Y., Chen, X., Sun, K., and Lai, Q. (2020). "Calibration and experiment of simulation parameters for *Panax notoginseng* seeds based on DEM," *Trans. Chinese Soc. Agric. Machinery* 51(02), 123-132. DOI: 10.6041 /j.issn.1000-1298.2020.02. 014

Zhang, T., Liu, F., Zhao, M., Liu, Y., Li, F., Ma, Q., Zhang, Y., and Zhou, P. (2017). "Measurement of physical parameters of contact between soybean seed and seed metering device and discrete element simulation calibration," *J. China Agric. University* 23(04), 120-127. DOI: 10.11841/j.issn.1007-4333.2017.09.11

Zhang, T., Liu, F., Zhao, M., Ma, Q., Wang, W., Fan, Q., and Yan, P. (2018). "Determination of corn stalk contact parameters and calibration of discrete element method simulation," *J. China Agric. University* 22(09), 86-92. DOI: 10.11841/j.issn.1007-4333.2018.04.15

Zhang, C., Du, W., Chen, Z., and Su, R. (2019). "The measurement of contact parameters of buckwheat rice screening material and discrete element simulation calibration," *Agric. Mech. Res.* 41(01), 46-51. DOI: 10.13427/j.cnki.njyi.2019.01.008

Zhang, T., Zhao, M. Q., Liu, F., Tian, H. Q., Wulan, T. Y., Yue, Y., and Li, D. P. (2020). " A discrete element method model of corn stalk and its mechanical characteristic parame ters," *BioResources* 15(4), 9337-9350. DOI: 10.15376/biores.15.4.9337-9350

Article submitted: July 29, 2022; Peer review completed: October 29, 2022; Revised version received and accepted: November 6, 2022; Published: November 15, 2022.
DOI: 10.15376/biores.18.1.400-416